



Contents lists available at [SciVerse ScienceDirect](http://www.sciencedirect.com)

# Dendrochronologia

journal homepage: [www.elsevier.de/dendro](http://www.elsevier.de/dendro)



## ORIGINAL ARTICLE

# Age-related drought sensitivity of Atlas cedar (*Cedrus atlantica*) in the Moroccan Middle Atlas forests

Juan Carlos Linares<sup>a,\*</sup>, Lahcen Taiqui<sup>b</sup>, Gabriel Sangüesa-Barreda<sup>c</sup>, José Ignacio Seco<sup>a</sup>,  
Jesús Julio Camarero<sup>c</sup>

<sup>a</sup> Departamento de Sistemas Físicos, Químicos y Naturales, Universidad Pablo de Olavide, Ctra. Utrera km. 1, E-41002 Sevilla, Spain

<sup>b</sup> Faculté des Sciences, Université Abdelmalek Essaadi, Mhannech II, 93002, B.P. 2121 Tétouan, Morocco

<sup>c</sup> ARAID, Instituto Pirenaico de Ecología (CSIC), Avda. Montañana 1005, Apdo. 202, E-50192 Zaragoza, Spain

## ARTICLE INFO

### Article history:

Received 8 December 2011

Accepted 27 August 2012

### Keywords:

*Cedrus atlantica*

Dendroecology

Drought

Growth–climate relationships

Linear mixed-effects models

Standardized precipitation index

## ABSTRACT

Age-related tree responses to climate change are still poorly understood at the individual tree level. In this paper, we seek to disentangle the relative contribution of tree age to growth decline and growth–climate relationships in Atlas cedar (*Cedrus atlantica* Manetti) trees at the Middle Atlas Mountains, northern Morocco. Dendrochronological methods were applied to quantify growth–climate relationships using tree-ring width indices (TRWi) calculated for cedars of two contrasting age groups (old trees, age  $\geq 150$  years; young trees, age  $< 150$  years). TRWi–climate relationships were assessed at the site and tree levels by using response functions and linear mixed-effects models, respectively. Growth of the studied Atlas cedars was negatively affected by recurrent droughts and by the steep temperature rise since the 1970s. Response functions and mixed-effects models indicated that the decline in tree growth was mainly explained by diminishing precipitation. The negative association between cedar growth and temperature was stronger in old than in young trees. Vulnerability to temperature-induced drought stress in old cedar trees may lead to an impending growth decline. We argue that the age dependence of growth sensitivity to drought must be quantified and considered at the individual tree level when predicting the future dynamics and persistence of cedar forests in the Moroccan Middle Atlas.

© 2012 Published by Elsevier GmbH. on behalf of Istituto Italiano di Dendrochronologia.

## Introduction

Drought-related tree growth decline and associated increased mortality risk are recurrent phenomena that have been reported in a variety of forest communities around the world (e.g., Dobbertin, 2005; van Mantgem et al., 2009; Allen et al., 2010; Linares and Camarero, 2012). Drought may intensify physiological stress on long-lived woody vegetation, leading to sudden growth reduction (Bigler et al., 2004; McDowell et al., 2008; Lloret et al., 2011; Hereş et al., 2012). Growth decline in response to severe droughts may trigger widespread mortality which can transform drought-sensitive pine, fir or cedar landscapes to more open stands dominated by other woody species more resistant to drought, including oaks (*Quercus* sp.) and junipers (*Juniperus* sp.), at regional to local scales (Allen and Breshears, 1998; Galiano et al., 2010; Gonzalez et al., 2010; Linares et al., 2011).

Radial growth can be used as a surrogate of the whole-tree carbon budget (e.g., Litton et al., 2007; Zweifel et al., 2010; but see also Rocha et al., 2006). Such use implies that tree-ring data provide valuable information about the effects of environmental change on forest productivity. Dendrochronology has long used tree-rings to better understand climate–growth relationships in trees within a site or across a region, with tree age often considered to contribute unwanted noise to the signal (Cook, 1985; Osborn et al., 1997; Vaganov et al., 2006). Thus, age-dependent effects often have not been taken into account in investigations of the interactions between climate change and tree growth decline (Voelker, 2011).

The most common approach in dendroecological studies to deal with age growth trends, i.e. the tendency of tree rings to get narrower as trees get bigger and older, is to detrend tree-ring width series by calculating ratios or differences between the raw data and fitted curves (e.g., negative linear or exponential curves) to obtain site mean chronologies averaging the indexed values across trees and for each year (Cook and Peters, 1981, 1997). Therefore, such pooled tree-ring indices do not account for the variance in climate–growth responses among trees. Moreover if the age growth trends of some trees covary with a given climatic

\* Corresponding author.

E-mail address: [jclinalc@upo.es](mailto:jclinalc@upo.es) (J.C. Linares).

trend, detrending would also remove part of the environmental signal of interest. Here, we combined both standard detrending methods, widely used among dendrochronologists, with linear mixed-effects models by multi-model selection criteria, to model, at an individual tree scale, age-dependent growth responses to local temperature and precipitation. We provide a novel advance for analyzing the effects of both climatic stress and intrinsic age effects on growth, using linear mixed-effects models to reproduce changes in tree-ring width indices at the individual tree level.

We focused on Atlas cedar (*Cedrus atlantica* Manetti) because it is an endemic and long-lived tree species, which is considered to be highly vulnerable to climatic warming and the related decrease in soil-water availability (Cheddadi et al., 2009; Linares et al., 2011). Since the early 1980s, severe droughts have been related to Atlas cedar growth decline and mortality (Bentouati, 2008; Mokrim, 2009; Allen et al., 2010), mainly in the mountainous xeric areas near the Sahara Desert (Chenchouni et al., 2008). The Atlas cedar growth decline seems to affect mainly old dominant trees, which suggests age/size-dependent tree responses to long-term changes in water availability (Linares et al., 2011).

We hypothesized that: (i) growth response to drought increases is modulated by inherent age-dependent sensitivity to temperature, precipitation and drought and (ii) age affects the vulnerability of tree species to climate-induced stress. To test these hypotheses, we investigated local climatic trends (temperature and precipitation) for the 20th century, and we measured tree-ring width and calculated tree-ring width indices from *C. atlantica* trees sampled in the Middle Atlas, northern Morocco. Our specific aims were: (i) to quantify the extent to which temperature, precipitation and drought drive the *C. atlantica* climate-growth patterns in trees of different ages and (ii) to evaluate whether age-dependent responses to climate could explain recent Atlas cedar growth decline. The fulfillment of these aims may shed light on the nature of age-dependent links between climate change and growth in trees. Furthermore they could allow evaluation of whether variables such as tree age are appropriate to forecast drought-induced forest decline.

## Methods

### Study species

Currently, the genus *Cedrus* includes three extant species native to the Mediterranean mountains (*C. atlantica* from Algeria and Morocco; *Cedrus libani* Rich. in Asia Minor; *Cedrus brevifolia* (Hooker fil.) Henry in Cyprus) and another one in the Himalaya (*Cedrus deodara* Don; Farjon, 2008). The Atlas cedar forests cover an area of over 130,000 ha (Cheddadi et al., 2009) distributed over Morocco (Rif, Middle Atlas and north-eastern High Atlas) and Algeria (Ouarsenis, Aurès and Djurdjura; see Linares et al., 2011). *C. atlantica* occurs at elevations of 1300–2600 m a.s.l., where the amount of annual rainfall ranges from 500 to 2000 mm and the minimum temperature of the coldest month ranges between  $-1^{\circ}\text{C}$  and  $-8^{\circ}\text{C}$  (Benabid, 1994; Mhirit, 1994). The Middle Atlas in northern Morocco contains about the 80% of the world's Atlas cedar forest area (ca. 100,000 ha; Benabid, 1994; Linares et al., 2011). The Atlas cedar has relatively wide tolerances with regard to climate and soil type. Middle Atlas cedar forests contain several evergreen (holm oak, *Quercus rotundifolia* Lam.; prickly juniper, *Juniperus oxycedrus* L.; European holly, *Ilex aquifolium* L.) and deciduous (*Acer opalus* Mill., *Crataegus laciniata* Ucria) tree and shrub species. The most abundant tree species, beside Atlas cedar, in the stands studied was *Q. rotundifolia* (Linares et al., 2011).

### Climate data

To quantify temperature and precipitation trends over the second half of the 20th century (period 1950–2006) we used local climatic data (monthly mean temperature and total precipitation) from the Ifrane meteorological station located about 14 km apart from the studied plots ( $33^{\circ}32'\text{N}$ ,  $5^{\circ}07'\text{W}$ , 1630 m, period 1958–2003 and estimated the other values through linear correlations using gridded regional data from the CRU TS 3.0 dataset produced by the Climate Research Unit (CRU, 2008). Although all correlations between local and regional data were highly significant, we only used the local dataset to model tree growth in further analyses (see Linares et al., 2011). The annual water budget was estimated by the Palmer drought severity index (PDSI) obtained from gridded regional data from the CRU TS 3.0 dataset (van der Schrier et al., 2006; CRU, 2008). Mean temperature and PDSI were standardized by subtracting the mean and dividing by the standard deviation:

$$Z_i = \frac{(x_i - \bar{x})}{\sigma}, \quad (1)$$

where  $Z_i$  expresses the  $x_i$  score distance from the  $x$  average ( $\bar{x}$ ) in standard deviation units ( $\sigma$ ).

To determine the severity and the rarity, in statistical terms, of extreme drought events, precipitation data were standardized by calculating the standardized precipitation index (SPI; McKee et al., 1993a). The SPI accounts for the frequency distribution of precipitation. Conceptually, the SPI also represents a z-score of an event, i.e. the number of standard deviations above or below the mean of that event, as has been defined in Eq. (1) for temperature and PDSI values. However, the SPI performs a pre-adjustment to this formulation because precipitation is usually positively skewed (Bordi et al., 2001). To adjust for this statistical bias in rainfall data, the precipitation data were transformed to a more normal distribution by applying the gamma function (see Appendix 1 for a detailed report about SPI computation).

### Dendrochronological methods

To quantify the growth patterns of *C. atlantica*, a total of 53 dominant and co-dominant trees were selected based on an extensive field survey within an area delimited by the following coordinates: latitude  $33^{\circ}24'40''$ – $33^{\circ}24'60''\text{N}$  and longitude  $5^{\circ}03'00''$ – $5^{\circ}08'40''\text{W}$ . The elevation varied from 1830 to 1890 m, i.e. near the lowermost elevation limit of the distribution of this species in the Middle Atlas (Benabid, 1994; see also Linares et al., 2011). All trees were located on limestone substrates. We selected and specifically sampled trees showing regular and straight boles, and we avoided those with asymmetrical or eccentric growth. We then extracted from two to four cores per tree at breast height (1.3 m) and always in a direction perpendicular to the terrain maximum slope using 40-cm or 60-cm long Pressler increment borers, depending on the diameter of the trees sampled. Bark and core length were measured in the field (as well as tree diameter). When the core did not reach the pith (ca. 10% of the cored trees), total tree age at coring height was thereafter estimated by linear regressions assuming an averaged growth rate for the missing innermost rings.

All cores were sanded with sandpapers of progressively finer grain until tree rings were clearly visible under a binocular microscope, and then were visually cross-dated. Tree-ring widths were measured to the nearest 0.001 mm using a LINTAB measuring device (Rinntech, Heidelberg, Germany), and cross-dating quality was checked using the COFECHA program (Holmes, 1983).

The trend due to the geometrical constraint of adding a volume of wood to a stem of increasing radius was corrected by

converting tree-ring widths into indices following the standard dendrochronological procedures based on detrending. For each individual tree, standardized tree chronologies were built from cross-dated ring-width series using the ARSTAN program by using a two-step detrending procedure (Cook, 1985). Negative exponential functions were first fitted to the series, and then a cubic smoothing spline with a 50% frequency response of 100 years was fitted. We acknowledge the fact that the applied detrending will limit our findings to inter-annual and decadal fluctuations. The detrended series were then standardized and transformed into dimensionless indices by dividing the observed by the expected values given by the functions. Then, autoregressive modeling was performed on each series to remove the serial correlation between tree-rings and to obtain residual series of tree-ring width indices (TRWi). We calculated chronologies at the individual level by averaging TRWi values for each tree. These data were used for individual climate-growth analyses (see “Linear mixed-effects models of TRWi at the individual tree level” section). To detect which were the main climatic drivers of growth at the population level we obtained a mean chronology of all trees by averaging the indexed values for each year using a bi-weight robust mean. We also obtained mean chronologies for the two age groups analyzed (old trees, age  $\geq 150$  years; young trees, age  $< 150$  years).

We related the mean site residual chronology calculated considering all trees to standardized monthly climate data (mean temperature, SPI, PDSI) for the period 1950–2006 using response functions. Response function coefficients were based on bootstrapped stepwise multiple regressions computed on the principal components of climatic variables (Fritts, 1976). The bootstrapped response function is a robust approach to test the significance of the regression climate-growth coefficients within a specific time period and avoids the spurious effects caused by the existence of collinearity among climatic variables. We calculated the response coefficients from September of the previous year (year  $t-1$ ) up to September of the year of tree-ring formation (year  $t$ ). Mean regression coefficients were regarded as significant ( $p < 0.05$ ) if they were at least twice their standard deviation after 999 bootstrapped iterations. Bootstrap response functions were calculated using the program Dendroclim2002 (Biondi and Waikul, 2004).

Dendrochronological statistics were calculated for the common period 1950–2009 to characterize the raw (MW, mean tree-ring width; SD, standard deviation; AC, first-order autocorrelation) and residual chronologies of the two age groups considered ( $ms_x$ , mean sensitivity;  $r_{bt}$ , mean between-trees correlation; EPS, expressed population signal; E1, percentage of variance explained by the first principal component; Fritts, 1976). The first-order autocorrelation of ring-width series (AC) measures the year-to-year growth similarity, whereas the mean sensitivity ( $ms_x$ ) of residual ring-width series quantifies the relative year-to-year variability in width of consecutive tree rings. Finally, the mean between-trees correlation ( $r_{bt}$ ) is a measure of the similarity in growth among trees, the expressed population signal (EPS) is a measure of the statistical quality of the mean site chronology as compared with a perfect infinitely replicated chronology, and the percentage of variance explained by the first principal component (E1) is an estimate of the common variability in growth among all trees.

#### Linear mixed-effects models of TRWi at the individual tree level

We fitted linear mixed-effects models using the *nlme* package in R software (R Development Core Team, 2012) to explain TRWi variability using mean monthly temperature, SPI, and PDSI from September of the previous year ( $t-1$ ) up to September of the year of tree-ring formation ( $t$ ) as explanatory variables. Climate

variables were included as fixed effects, and each tree was included as a random effect based on the following equation:

$$TRWi = I + (\text{temperature, SPI, PDSI}) + \varepsilon \quad (2)$$

where  $I$  is the intercept; temperature, SPI and PDSI represent the standardized monthly data for these variables; and  $\varepsilon$  is the error component (Pinheiro et al., 2011). The covariance parameters were estimated using the restricted maximum likelihood method, which estimates the parameters by minimizing the likelihood of residuals from the fitting of the fixed-effects portion of the model (see further details in Pinheiro et al., 2011). We used an information-theoretic approach for multi-model selection, based on the Akaike information criterion (AIC; Akaike, 1974) corrected for small sample sizes (AICc). The AIC combines the measure of goodness of fit with a penalty term based on the number of parameters used in the model. Significant variables were selected using a backward step-wise procedure based on AICc. We considered models with substantial support to be those in which the  $\Delta AIC$  (i.e. the difference of AICc between models) was  $< 2$  (see Burnham and Anderson, 2002).

Growth-climate linear mixed-effects models were fitted using all trees, i.e. not differentiating age classes. Thereafter, we explored the age distribution of the sampled trees and we defined two age classes accounting for a reasonable compromise between adequate sample size and sufficient data discrimination. Differences in variance explained by temperature, SPI and PDSI were computed between age classes by one-way ANOVA comparing variance explained for each individual tree.

## Results

### Climate trends

Linear regression analyses performed over the mean temperature series showed a significant increase ( $p < 0.001$ ; Fig. 1), which accounted for a warming of  $+1.6^\circ\text{C}$  on average for the 1958–2003 span, being highest from March to June (data not shown). The annual SPI showed a marginally significant ( $p = 0.06$ ) negative trend, which accounted for a decrease of  $-364$  mm in the raw annual precipitation for the 1958–2003 span (i.e. an approximate 28% reduction in the total annual precipitation). The greatest precipitation decrease was found in early spring (March and April, data not shown). Extreme drought events were more pronounced towards the end of the 20th century (Fig. 1). PDSI showed a notable decrease ( $p < 0.001$ , Fig. 1) as a result of the above indicated trends corresponding to increasing mean temperatures and decreasing total precipitation.

### Growth-climate relationships

The highest and most significant response coefficients were obtained for current May SPI and April–August PDSI, whereas the previous September PDSI showed a negative association with TRWi (Fig. 2). The model with highest explanatory value, based on temperature variables, included a negative effect for previous September and current May and June, while previous October and current April and September mean temperature showed a positive effect (Table 1). This model accounted for 12.5% of the TRWi variance. PDSI accounted for 24.7% of the TRWi variance, with previous October and current March and September showing a negative effect on TRWi (i.e. higher TRWi as drought increases during these months), while current May and August showed a positive effect (i.e. higher TRWi as drought decreases during these months). SPI variables showed always positive effects on TRWi and accounted for 24.8% of growth variance. SPI-based models rendered slightly



**Table 1**  
Selection criteria for linear mixed-effects models of tree ring-width indices (TRWi) considering all Atlas cedars trees (young and old trees) together ( $n = 4731$  rings; 53 trees). A null model considering TRWi as a constant was also tested.

Model	K	AICc	$\Delta i$	$L(gi/x)$	Variance explained (%)
SPINp + SPIJA + SPIMR + SPIAP + SPIMY	7	363.50	0.00	1.00	24.8
POp + PMR + PMY + PAU + PS	7	366.40	2.90	0.23	24.7
TSp + TOP + TAP + TMY + TJN + TS	8	1072.72	709.22	0.00	12.5
Null model	2	1363.89	1000.40	0.00	nc

Abbreviations:  $k$ , number of parameters included in the model (number of explaining variables plus one constant plus the error);  $\Delta i$ , difference in AICc (Akaike information criterion corrected for small samples) with respect to the best model;  $L(gi/x)$ , Likelihood of a model  $gi$  given the data  $y$ ; nc, non-computed value. The symbols (+) and (–) indicate positive and negative effects, respectively, for the following climatic variables: SPINp standardized precipitation index (SPI) of previous November (+); SPIJA, January SPI (+); SPIMR, March SPI (+); SPIAP, April SPI (+); SPIMY, May SPI (+). POp, previous October Palmer drought severity index (PDSI) (–); PMR, March PDSI (–); PMY, May PDSI (+); PAU, August PDSI (+); PS, September PDSI (+). TSp, previous September temperature (–); TOP, previous October temperature (+); TAP, April temperature (+); TMY, May temperature (+); TJN (–), June temperature (–); TS, September temperature (+).

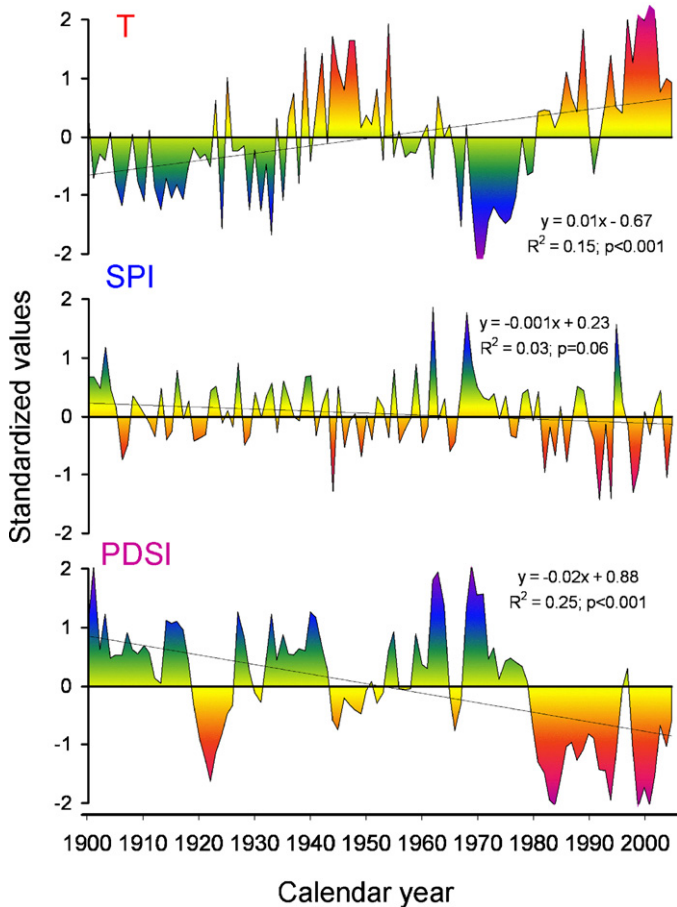


**Fig. 1.** Standardized mean annual temperature ( $T$ ), standardized precipitation index (SPI) and standardized Palmer drought severity index (PDSI) in the study area for the period 1901–2006. We used local climatic data from the Ifrane meteorological station for the period 1958–2003 and estimated the other values through linear correlations calculated between local and gridded regional data (CRU TS 3.0 dataset). Although all correlations between local and regional data were highly significant ( $p < 0.001$ ), we only used the local dataset to model tree growth in further analyses.

higher explanatory value of TRWi variability than PDSI-based models (Table 1). SPI of previous November and current January, March, April and May were selected in the model with highest explanatory value.

**Age-related drought sensitivity of Atlas cedar**

Year-to-year serial correlation (AC) was higher in old than in young trees, whereas the reverse was observed in the case of mean ring-width (Table 2). The relative year-to-year variability in width

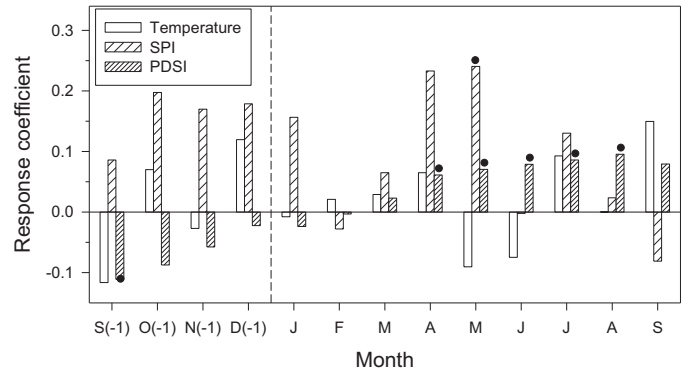


**Fig. 2.** Response function computed on tree-ring width indices based on 53 Atlas cedar trees. Significant response coefficients ( $p < 0.01$ ) are indicated by filled symbols located above bars. The tested monthly climatic variables are the mean monthly temperature, the monthly standardized precipitation index (SPI) and the monthly Palmer drought severity index (PDSI). The analyzed temporal window includes the period from September (–1) of the previous year up to September of year of tree-ring formation.

of consecutive tree rings ( $ms_x$ ) and the similarity in growth among trees ( $r_{bt}$ ) were similar between the two age classes.

Trees were grouped into cedars younger (young;  $n = 30$ ) and older (old;  $n = 23$ ) than 150 years, respectively (Fig. 3). Young and

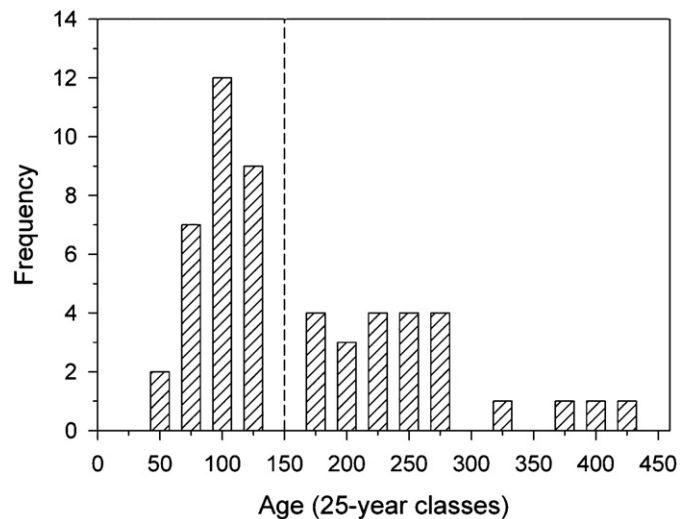


**Fig. 3.** Frequency distribution of age estimated at 1.3 m (25-year classes) of sampled Atlas cedars (*Cedrus atlantica*) from the Moroccan Middle Atlas. The vertical dotted line separates the two age groups analyzed, i.e. trees younger and older than 150 years, respectively. These two groups were used for further comparisons in growth–climate relationships.

**Table 2**  
Dendrochronological statistics calculated for the ring-width chronologies of each cedar group for the common period 1950–2009.

Group	No. trees/radii	Raw tree-ring data			Residual chronology			
		MW (mm)	SD (mm)	AC	ms <sub>x</sub>	r <sub>bt</sub>	EPS	E1 (%)
Young	30/60	1.89a	0.99	0.76a	0.20	0.51	0.89	56.38
Old	23/50	1.09b	0.92	0.87b	0.17	0.49	0.86	40.67

Abbreviations: MW, mean ring-width; SD, ring-width standard deviation; AC, first-order autocorrelation (a measure of the year-to-year growth similarity); ms<sub>x</sub>, mean sensitivity (a measure of the year-to-year variability in width of consecutive rings); r<sub>bt</sub>, mean between-trees correlation; EPS, expressed population signal (a measure of the statistical quality of the mean site chronology as compared with a perfect infinitely replicated chronology); E1, variance explained by the first principal component (an estimate of the common variability in growth among all trees at each site).

Comparisons for selected statistics were based on one-way ANOVA and different letters represent significant ( $p < 0.05$ ) differences between young and old cedars.

old trees had mean ± standard deviation diameters at 1.3 m of 43.14 ± 9.64 cm and 108.11 ± 48.19 cm, and mean ages of 86 ± 18 and 243 ± 72 years, respectively.

Atlas cedar showed severe growth reductions during the past century in 1979–1981, 1995, 1999 and 2005 (Fig. 4). The year-to-year TRWi variability increased in the 1990s and 2000s as compared with previous decades and the most extreme growth indices observed in these decades were more frequent in young than in old trees (Fig. 4). Old trees showed higher responsiveness to temperature than the young ones (18% of explained variance vs. 9%, respectively; Fig. 4). At the individual tree level, the variance explained by temperature was significantly higher for old trees than for young ones (Fig. 5), while young trees showed slightly higher variance explained by precipitation than old ones (marginally significant;  $p = 0.09$ ), and no significant differences among age classes were found for PDSI.

**Discussion**

*Drought induction of Atlas cedar growth decline*

We hypothesized that tree vulnerability to climate change could be modulated by age-dependent growth sensitivity to drought, providing valuable information to infer the underlying

mechanisms leading to growth decline at the individual tree level. Overall, our results support the contention that rising spring and summer temperatures and decreasing rainfall from winter to early summer will magnify Atlas cedar growth decline (Aussenac and Finkelstein, 1983; Till, 1987; Mokrim, 2009). This conclusion may be also applied to other drought-triggered growth declines which have been reported in other Mediterranean mountain conifers such as *Pinus sylvestris* (Martínez-Vilalta et al., 2008; Hereş et al., 2012), *Pinus nigra* (Linares and Tiscar, 2010; Candel-Pérez et al., 2012), *Abies alba* and *Abies pinsapo* (Camarero et al., 2011; Linares and Camarero, 2012). However, we also found that the effects of rising temperature on *C. atlantica* growth decline are age-dependent, i.e. that the negative effects of temperature warming on growth are stronger in old than in young trees.

In the Middle Atlas, about 23% of the area covered by cedars showed growth decline and dieback symptoms (defoliation, increased mortality) after recent severe droughts (Bentouati,

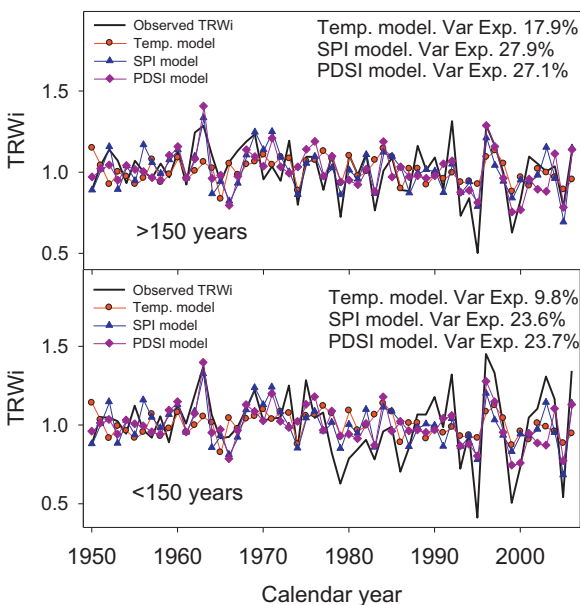


**Fig. 4.** Observed and predicted changes in tree-ring width index (TRWi) of cedars younger (young;  $n = 30$  trees) and older (old;  $n = 23$  trees) than 150 years from the Moroccan Middle Atlas. Standardized mean annual temperature (temp. model, ●), standardized precipitation index (SPI model, ▲) and standardized Palmer drought severity index (PDSI model, ◆) were tested as predictors by using linear mixed-effects models.

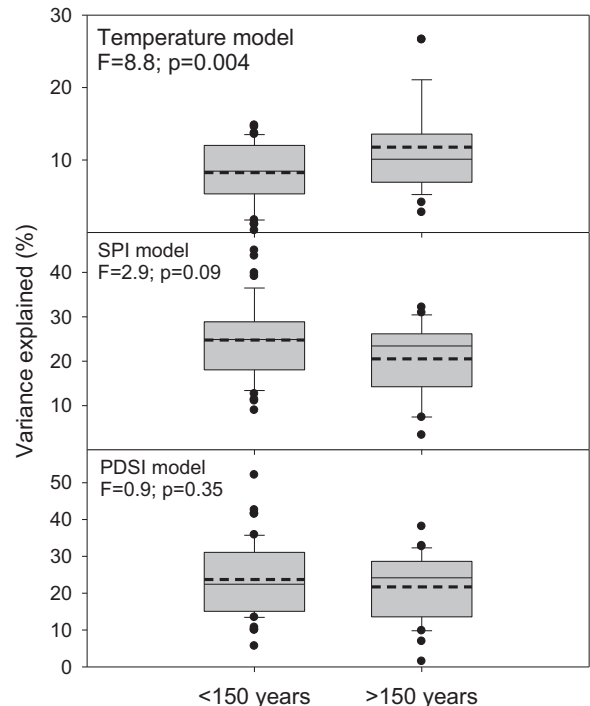


**Fig. 5.** Tree ring-width index variance explained by the climatic models (see Table 1) based on standardized monthly mean annual temperature, monthly precipitation index (SPI) and Palmer drought severity index (PDSI) computed by linear mixed-effects models. The variances explained for cedars younger (young;  $n = 30$  trees) and older (old;  $n = 23$  trees) than 150 years were compared using ANOVA tests. In the box-plot figure, error bars represent the 5th and 95th percentiles; boxes represent the standard errors; solid lines represent the median; dashed lines are the means; and points are outliers.  $F$  test values and significance levels ( $p$ ) are indicated for each climatic variable.

2008; Mokrim, 2009; Allen et al., 2010; Linares et al., 2011). Indeed, we found severe growth reductions during the past century in 1979–1981, 1995, 1999 and 2005. In a longer temporal context, several reconstructions suggest that during the late 20th century Morocco underwent some of the most severe droughts since at least the mid 15th century (Till and Guiot, 1999; Esper et al., 2007; Touchan et al., 2008). In our study area, growth reductions of cedars occurred mainly since 1978, and were related to severe droughts and temperature rise as reflected in the available local climatic records (Mokrim, 2009; Linares et al., 2011).

Growth and monthly precipitation showed significant positive correlations, based on linear mixed-effects models, from November of the previous year to the current May, in agreement with response function and previous growth–climate analyses, illustrating how precipitation is the main limiting factor for the growth of Atlas cedar (Aussenac and Finkelstein, 1983; Till, 1987), as in other cedar species such as *C. libani* (Akkemik, 2003), *C. brevifolia* (Touchan et al., 2005), and *C. deodara* (Borgaonkar et al., 1999). However, our growth–temperature correlations contrast with those of Till (1987), who reported a positive effect of January mean temperature for Atlas cedar based on response functions computed for the period 1941–1970. It should be noted that the Till (1987) study included Atlas cedar populations from the Rif, Middle Atlas and High Atlas Mountains at elevations ranging from 1400 to 2600 m. Our analyses cover the second half of the 20th century, for which the temperature trend was characterized by a sharp rise, mainly since the 1970s onwards. In addition, our study focuses on Atlas cedar forests near the lowermost elevation limit of the distribution of this species in the Middle Atlas (Benabid, 1994). We expect that low-elevation cedar stands exhibit a lower positive effect of winter-to-spring temperatures on growth than high-elevation stands subjected to cold conditions.

In conifers, severe drought stress affects processes related to cambium activity and xylogenesis, including carbon sink–source trade-offs mediated by xylem and phloem formation (Vaganov et al., 2006). Warming-induced drought stress may alter the partitioning of newly fixed carbon in such a way that less carbon is diverted to secondary growth and wood formation thus negatively affecting hydraulic conductivity (McDowell et al., 2008). Our results agree with the first reasoning since we found a negative association between secondary growth and May–June temperature, the period when Atlas cedar presents maximum radial-growth rates (Aussenac and Finkelstein, 1983). In addition, the negative effect on growth observed for prior September temperature could be related to stomatal control of water loss in late summer to early autumn of the year before tree-ring formation, which may reduce carbohydrate synthesis and storage, increase carbon losses through enhanced respiration, and decrease wood formation in spring (McDowell et al., 2008).

The pronounced decrease in growth of the studied Atlas cedar stands since the early 1980s coincided with the local rise of air temperatures, and the occurrence of severe drought events, and it is also in agreement with long-term drought reconstructions in Morocco (Esper et al., 2007). As stated above, this apparently drought-triggered growth decline may be linked to the dieback of cedar forests in the Moroccan Middle Atlas (Linares et al., 2011). However it should be also noted that, besides drought stress, other factors may also explain the observed growth patterns. For instance, local anthropogenic disturbances (overgrazing, pruning, logging), crown defoliation by processionary caterpillars (*Thaumetopoea bonjeani* and *Thaumetopoea pityocampa*) and cedar bark stripping by Barbary Macaques (*Macaca sylvanus*) seem to be interacting with climate-driven factors on recent Atlas cedar decline (Camperio Ciani et al., 2001; Linares et al., 2011). Therefore they

may be involved in the occurrence of alternating phases of growth reduction and recovery in Atlas cedar forests.

#### Age-related drought sensitivity of Atlas cedar

We demonstrate here that Atlas cedar growth–climate relationships are age-dependent, as has been shown in other tree species growing in harsh environments such as subalpine forests (see for instance Carrer and Urbinati, 2004). This finding suggests the existence of age-related changes in endogenous parameters possibly linked to the hydraulic status and the tree carbon balance. Our results support the idea that rising spring to summer temperatures become more limiting for growth as trees become older.

The higher xylem hydraulic safety found in old trees as compared with young ones (Magnani et al., 2000; Domec and Gartner, 2002) suggests the former display lower sensitivity to water deficit than the latter ones (Ryan et al., 1997). However, increased size and structural complexity augment maintenance respiration costs (Hunt et al., 1999) and reduce the efficiency of the hydraulic pathway, which may explain the observed growth reduction and the increase in temperature sensitivity (Ryan and Yoder, 1997). Such ontogenetic changes affect xylogenesis (Rossi et al., 2008) and modify growth–climate relationships (Carrer and Urbinati, 2004). Additionally, old and usually large and dominant trees should display improved growth conditions by lowering sensitivity to competition despite increasing tree height leads to decreasing hydraulic conductance (Domec and Gartner, 2002). Nevertheless, the stronger growth response to temperature in old than in young trees might be due to a difference in canopy temperature and thus vapour pressure deficit given that usually canopies of old trees are exposed to more light than canopies of young trees (Bond, 2000).

Increases in hydraulic resistance could reduce the supply of water for transpiration and induce earlier stomatal closure to prevent xylem dysfunction through cavitation (Ryan et al., 2006), which in turn would decrease photosynthetic rates in old trees as compared with younger trees (Yoder et al., 1994; Bond, 2000). If old trees lose hydraulic conductivity throughout their trunks, they would need a larger sapwood area to maintain the same water flux for a given water potential gradient. Then, increased sapwood area would mean a larger number of parenchyma cells and, hence, higher respiration rates and also increased temperature sensitivity (Domec and Gartner, 2002; Phillips et al., 2002).

Although PDSI did not show a significant age effect, as Esper et al. (2007) also noticed, young Atlas cedar trees showed slightly higher precipitation sensitivity than old ones (but the difference was only marginally significant), and could be more susceptible than the old ones to increased water deficit if the summer drought season becomes longer or more intense due to their limited root system (i.e. poor access to deeper water) and inability to induce stomatal closure and conserve water under moderate levels of vapour-pressure deficit (Wharton et al., 2009). Consistent with this hypothesis, the old trees may be slightly less sensitive than young ones to water availability due to contrasting wood anatomy and xylem function (lower hydraulic conductance and higher xylem safety in older trees; see Domec and Gartner, 2002; Kolb et al., 2007). However, other authors have found few evidence supporting age effects on the climate signal portrayed by tree rings and thus they recommended increasing sample replication when comparing young and old trees (see Esper et al., 2008).

#### Conclusions

The growth of cedars has progressively declined as aridity has increased in the Moroccan Middle Atlas. Temperature-induced



drought stress appears to become increasingly limiting as cedars age, whereas decreasing precipitation exerts a great impact on radial growth in both young than in old trees. This contrasting age-dependent climatic sensitivity may significantly impact future forest dynamics in the Middle Atlas at regional scales, since both a warming trend and a precipitation decline have been forecasted for upcoming decades. Our findings bear implications for Atlas cedar persistence in the Middle Atlas because ongoing decline of low-density cedar stands may accelerate soil erosion and their replacement by more drought-resistant species as *Q. rotundifolia*. We argue that the age dependence of growth sensitivity to temperature must be explicitly considered at the individual tree level for understanding and predicting the future responses of forests to climate warming.

**Acknowledgements**

J.C. Linares and L. Taïqui received financial support for this work from the Spanish Agency for International Cooperation and Develop (AECID), project A/024752/09. J.C. Linares is grateful to J.A. Carreira (Univ. Jaén) for providing additional support. L. Taïqui is grateful to M. Jabrane (Univ. Tetouan) and M. Benzyane, Ex-Director of the National Centre of Forest Research in Morocco, for providing the climatic data of Ifrane. J.J. Camarero acknowledges the financial support of ARAID and collaborative efforts within the Globimed network ([www.globimed.net](http://www.globimed.net)). We thank three anonymous reviewers for their comments which helped to improve a previous version of the manuscript.

**Appendix 1.. standardized precipitation index (SPI)**

To determine the severity and the statistical rarity of extreme drought events, precipitation data was standardized by calculating the standardized precipitation index (SPI) for the Ifrane meteorological station. The spatial and temporal dimensions of drought events create problems in generating a drought index because not only must an anomaly be normalized with respect to location, but the anomaly must also be normalized in time if it is to produce a meaningful estimate of drought. The SPI accomplishes both. The SPI is normalized to a station location because it accounts for the frequency distribution of precipitation as well as the accompanying variation at the station. Additionally, the SPI is normalized in time because it can be computed at any number of time scales, depending upon the impacts of interest to the analyst. Conceptually, the SPI represents a z-score, or the number of standard deviations above or below that an event is from the mean:

$$Z_i = \frac{(x_i - \bar{x})}{\sigma}$$

where  $Z_i$  expresses the  $x_i$  score's distance from the  $x$  average ( $\bar{x}$ ) in standard deviation units ( $\sigma$ ).

However, the SPI perform a pre-adjustment to this standard formulation due to precipitation is typically positively skewed. To adjust for this mathematical rainfall feature, the precipitation data is transformed to a more normal distribution by applying the gamma function (McKee et al., 1993b; Edwards and McKee, 1997; Bordi et al., 2001).

The gamma distribution is defined by its frequency or probability density function:

$$g(x) = \begin{cases} 1 \\ \beta^\alpha \Gamma(\alpha) \end{cases} x^{\alpha-1} e^{-x/\beta} \quad \text{for } x > 0 \tag{A1}$$

where  $\alpha > 0$  is a shape parameter;  $\beta > 0$  is a scale parameter;  $x > 0$  is the precipitation amount;  $\Gamma(\alpha)$  is the gamma function:

$$\Gamma(\alpha) = \int_0^\infty y^{\alpha-1} e^{-y} dy \tag{A2}$$

Computation of the SPI involves fitting a gamma probability density function to a given frequency distribution of precipitation totals for a station. The alpha and beta parameters of the gamma probability density function are estimated for each station, for each time scale of interest (seasonal, annual, etc.), and for each month of the year. The maximum likelihood solutions are used to optimally estimate  $\alpha$  and  $\beta$  as follows:

$$\hat{\alpha} = \frac{1}{4A} \left( 1 + \sqrt{1 + \frac{4A}{3}} \right) \tag{A3}$$

$$\hat{\beta} = \frac{\bar{x}}{\hat{\alpha}} \tag{A4}$$

where

$$A = \ln(\bar{x}) - \frac{\sum \ln(x)}{n} \tag{A5}$$

$n$  = number of precipitation observations.

The resulting parameters are then used to find the cumulative probability of an observed precipitation event for the given month and time scale for the station in question. The cumulative probability is given by:

$$G(x) = \int_0^x g(x) dx = \frac{1}{\hat{\beta}^{\hat{\alpha}} \Gamma(\hat{\alpha})} \int_0^x x^{\hat{\alpha}-1} e^{-x/\hat{\beta}} dx \tag{A6}$$

Letting  $t = x/\hat{\beta}$ , this equation becomes the incomplete gamma function:

$$G(x) = \frac{1}{\Gamma(\hat{\alpha})} \int_0^x t^{\hat{\alpha}-1} e^{-t} dx \tag{A7}$$

Since the gamma function is undefined for  $x=0$  and a precipitation distribution may contain zeros, the cumulative probability becomes:

$$H(x) = q + (1 - q)G(x) \tag{A8}$$

where  $q$  is the probability of a zero. If  $m$  is the number of zeros in a precipitation time series,  $q$  can be estimated by  $m/n$ .

The cumulative probability,  $H(x)$ , is then transformed to the standard normal random variable  $Z$  with mean zero and variance of one (see Eq. (1)) as follows:

$$Z = \text{SPI} = - \left( t - \frac{c_0 + c_1 + c_2 t^2}{1 + d_1 t + d_2 t^2 + d_3 t^3} \right) \quad \text{for } 0 < H(x) \leq 0.5 \tag{A9}$$

$$Z = \text{SPI} = + \left( t - \frac{c_0 + c_1 + c_2 t^2}{1 + d_1 t + d_2 t^2 + d_3 t^3} \right) \quad \text{for } 0.5 < H(x) < 1.0 \tag{A10}$$

where

$$t = \sqrt{\ln \left( \frac{1}{(H(x))^2} \right)} \quad \text{for } 0 < H(x) \leq 0.5 \tag{A11}$$

$$t = \sqrt{\ln \left( \frac{1}{(1.0 - H(x))^2} \right)} \quad \text{for } 0.5 < H(x) < 1.0 \tag{A12}$$

$$c_0 = 2.515517, \quad c_1 = 0.802853, \quad c_2 = 0.010328, \quad d_1 = 1.432788, \\ d_2 = 0.189269 \text{ and } d_3 = 0.001308.$$

## References

- Akaike, H., 1974. A new look at statistical model identification. *IEEE Transactions on Automatic Control* 19, 716–722.
- Akkemik, Ü., 2003. Tree rings of *Cedrus libani* at the northern boundary of its natural distribution. *IAWA Journal* 24, 63–73.
- Allen, C.D., Breshears, D.D., 1998. Drought-induced shift of a forest-woodland ecotone: rapid landscape response to climate variation. *Proceedings of the National Academy of Sciences of the United States of America* 95, 14839–14842.
- Allen, C.D., Macalady, A.K., Chenchouni, H., Bachelet, D., McDowell, N., Vennetier, M., Kitzberger, T., Rigling, A., Breshears, D.D., Hogg, E.H., Gonzalez, P., Fensham, R., Zhang, Z., Castro, J., Demidova, N., Lim, J.-H., Allard, G., Running, S.W., Smerci, A., Cobb, N., 2010. A global overview of drought and heat-induced tree mortality reveals emerging climate change risks for forests. *Forest Ecology and Management* 259, 660–684.
- Aussenac, G., Finkelstein, D., 1983. Influence de la sécheresse sur la croissance et la photosynthèse du Cèdre. *Annales des Sciences Forestières* 40, 67–77.
- Benabid, A., 1994. Biogéographie phytosociologie et phytodynamique des cédraies de l'Atlas (*Cedrus atlantica*, Manetti). Le cèdre de l'Atlas. Actes du séminaire international sur le cèdre de l'Atlas. *Annales Recherche Forestière au Maroc* 27, 62–76.
- Bentouati, A., 2008. La situation du cèdre de l'Atlas en Algérie. *Foret Méditerranéen* 29, 203–208.
- Bigler, C.J., Gricar, J., Bugmann, H., Cufar, K., 2004. Growth patterns as indicators of impending tree death in silver fir. *Forest Ecology and Management* 199, 183–190.
- Biondi, F., Waikul, K., 2004. DENDROCLIM2002: a C++ program for statistical calibration of climate signals in tree-ring chronologies. *Computers and Geosciences* 30, 303–311.
- Bond, B.J., 2000. Age-related changes in photosynthesis of woody plants. *Trends Plant Sciences* 5, 349–353.
- Bordi, I., Frigio, S., Parenti, P., Speranza, A., Sutera, A., 2001. The analysis of the Standardized Precipitation Index in the Mediterranean area: large-scale patterns. *Annali di Geofisica* 44, 965–978.
- Borgaonkar, H.P., Pant, G.B., Kumar, K.R., 1999. Tree-ring chronologies from western Himalaya and their dendroclimatic potential. *IAWA Journal* 20, 295–309.
- Burnham, K.P., Anderson, D.R., 2002. *Model Selection and Multimodel Inference*. Springer-Verlag, New York, 488 pp.
- Camarero, J.J., Bigler, C.J., Linares, J.C., Gil-Pelegrín, E., 2011. Synergistic effects of past historical logging and drought on the decline of Pyrenean silver fir forests. *Forest Ecology and Management* 262, 759–769.
- Camperio Ciani, A., Martinoli, C., Capiluppi, C., Arahou, M., Mouna, M., 2001. Effects of water availability and habitat quality on bark-stripping behavior in Barbary macaques. *Conservation Biology* 15, 259–265.
- Candel-Pérez, D., Linares, J.C., Viñegla, B., Lucas-Borja, M.E., 2012. Assessing climate-growth relationships under contrasting stands of co-occurring Iberian pines along an altitudinal gradient. *Forest Ecology and Management* 274, 48–57.
- Carrer, M., Urbinati, C., 2004. Age-dependent tree ring growth responses to climate of *Larix decidua* and *Pinus cembra* in the Italian Alps. *Ecology* 85, 730–740.
- Cheddadi, R., Fady, B., François, L., Hajar, L., Suc, J.-P., Huang, K., Demateau, M., Vendramin, G., Ortú, E., 2009. Putative glacial refugia of *Cedrus atlantica* deduced from quaternary pollen records and modern genetic diversity. *Journal of Biogeography* 36, 1361–1371.
- Chenchouni, H., Abdelkrim, S.B., Athmane, B., 2008. The deterioration of the Atlas cedar, *Cedrus atlantica*, in Algeria. In: *International Conference Adaptation of Forests and Forest Management to Changing Climate with Emphasis on Forest Health: A Review of Science, Policies, and Practices*. FAO/IUFRO, Umeå, Sweden, 25–28 August 2008.
- Cook, E.R., 1985. A time series analysis approach to tree ring standardization. PhD Dissertation. University of Arizona, Tucson, Arizona, 171 pp.
- Cook, E.R., Peters, K., 1981. The smoothing spline: a new approach to standardizing forest interior tree-ring width series for dendroclimatic studies. *Tree-Ring Bulletin* 4, 45–53.
- Cook, E.R., Peters, K., 1997. Calculating unbiased tree-ring indices for the study of climatic and environmental change. *The Holocene* 7, 361–370.
- CRU, 2008. University of East Anglia Climate Research Unit (CRU). CRU Datasets, [Internet]. British Atmospheric Data Centre, 2008, 16 March 2012. Available from <http://badc.nerc.ac.uk/data/cru>
- Dobbertin, M., 2005. Tree growth as indicator of tree vitality and of tree reaction to environmental stress: a review. *European Journal of Forest Research* 124, 319–333.
- Domec, J.C., Gartner, B.L., 2002. Age- and position-related changes in hydraulic versus mechanical dysfunction of xylem: inferring the design criteria for Douglas-fir wood structure. *Tree Physiology* 22, 91–104.
- Edwards, D.C., McKee, T.B., 1997. Characteristics of 20th Century Drought in the United States at Multiple Time Scales. Fort Collins, Colorado, Department of Atmospheric Science, Colorado State University, Colorado, USA, 155 pp.
- Esper, J., Frank, D.C., Büntgen, U., Verstege, A., Luterbacher, J., Xoplaki, E., 2007. Long-term drought severity variations in Morocco. *Geophysical Research Letters* 34, L17702.
- Esper, J., Niederer, R., Bebi, P., Frank, D.C., 2008. Climate signal age effects – evidence from young and old trees in the Swiss Engadin. *Forest Ecology and Management* 255, 3783–3789.
- Farjon, A., 2008. *A Natural History of Conifers*. Timber Press, Portland, 304 pp.
- Fritts, H.C., 1976. *Tree Rings and Climate*. Academic Press, London, 567 pp.
- Galiano, L., Martínez-Vilalta, J., Lloret, F., 2010. Drought-induced multifactor decline of Scots pine in the Pyrenees and potential vegetation change by the expansion of co-occurring oak species. *Ecosystems* 13, 978–991.
- Gonzalez, P., Neilson, R.P., Drapek, R.J., 2010. Global patterns in the vulnerability of ecosystems to vegetation shifts due to climate change. *Global Ecology and Biogeography* 19, 755–768.
- Hereş, A.M., Martínez-Vilalta, J., López, B.C., 2012. Growth patterns in relation to drought-induced mortality at two Scots pine (*Pinus sylvestris* L.) sites in NE Iberian Peninsula. *Trees* 26, 621–630.
- Holmes, R.L., 1983. Computer-assisted quality control in tree-ring dating and measurement. *Tree-Ring Bulletin* 43, 68–78.
- Hunt, E.R., Lavigne, M.B., Franklin, S.E., 1999. Factors controlling the decline of net primary production with stand age for balsam fir in Newfoundland assessed using an ecosystem simulation model. *Ecological Modelling* 122, 151–164.
- Kolb, T.E., Agee, J.K., Fule, P.Z., McDowell, N.G., Pearson, K., Sala, A., Waring, R.H., 2007. Perpetuating old ponderosa pine. *Forest Ecology and Management* 249, 141–157.
- Linares, J.C., Taïqui, L., Camarero, J.J., 2011. Increasing drought sensitivity and decline of Atlas cedar (*Cedrus atlantica*) in the Moroccan Middle Atlas forests. *Forests* 2, 777–796.
- Linares, J.C., Tiscar, P.A., 2010. Climate change impacts and vulnerability of the southern populations of *Pinus nigra* subsp. *salzmannii*. *Tree Physiology* 30, 795–806.
- Linares, J.C., Camarero, J.J., 2012. Growth patterns and sensitivity to climate predict silver fir decline in the Spanish Pyrenees. *European Journal of Forest Research* 131, 1001–1012.
- Litton, C., Raich, J.W., Ryan, M.G., 2007. Carbon allocation in forest ecosystems. *Global Change Biology* 13, 2089–2109.
- Lloret, F., Keeling, E.G., Sala, A., 2011. Components of tree resilience: effects of successive low-growth episodes in old ponderosa pine forests. *Oikos* 120, 1909–1920.
- Magnani, F., Mencuccini, M., Grace, J., 2000. Age-related decline in stand productivity: the role of structural acclimation under hydraulic constraints. *Plant, Cell and Environment* 23, 251–263.
- Martínez-Vilalta, J., López, B.C., Adell, N., Badiella, L., Ninyerola, M., 2008. Twentieth century increase of Scots pine radial growth in NE Spain shows strong climate interactions. *Global Change Biology* 14, 2868–2881.
- McDowell, N., Pockman, W.T., Allen, C.D., Breshears, D.D., Cobb, N., Kolb, T., Sperry, J., West, A., Williams, D., Yepez, E.A., 2008. Mechanisms of plant survival and mortality during drought: why do some plants survive while others succumb to drought? *New Phytologist* 178, 719–739.
- McKee, T.B., Doesken, N.J., Kleist, J., 1993. The relationship of drought frequency and duration to time scales. In: *Eighth Conference on Applied Climatology*. American Meteorological Society, Anaheim, pp. 179–184.
- McKee, T.B., Doesken, N.J., Kleist, J., 1993b. Drought monitoring with multiple timescales. Paper presented at the Preprints, Eighth Conference on Applied Climatology, Anaheim, California, USA, pp. 233–236.
- Mhirit, O., 1994. Le cèdre de l'Atlas (*Cedrus atlantica* Manetti). Présentation générale et état des connaissances à travers le réseau Silva Méditerranée 'Le Cèdre'. *Annales de la Recherche Forestière au Maroc* 27, 4–21.
- Mokrim, A., 2009. Dépérisement du cèdre de l'Atlas: Ambiance climatique et bilan de la croissance radiale. *Annales de la Recherche Forestière au Maroc* 41, 48–68.
- Osborn, T.J., Briffa, K.R., Jones, P.D., 1997. Adjusting variance for sample size in tree-ring chronologies and other regional mean time series. *Dendrochronologia* 15, 89–99.
- Phillips, N., Bond, B.J., McDowell, N.G., Ryan, M.G., 2002. Canopy and hydraulic conductance in young, mature and old Douglas fir trees. *Tree Physiology* 22, 205–211.
- Pinheiro, J., Bates, D., DebRoy, S., Sarkar, D., 2011. nlme: Linear and Nonlinear Mixed Effects Models. R Package Version 3.1–92.
- R Development Core Team, 2012. R: A Language and Environment for Statistical Computing. R Foundation for Statistical Computing, Vienna, Austria.
- Rocha, A.V., Goulden, M.L., Dunn, A.L., Wofsy, S.C., 2006. On linking interannual tree ring variability with observations of whole-forest CO<sub>2</sub> flux. *Global Change Biology* 12, 1378–1389.
- Rossi, S., Deslauriers, A., Anfodillo, T., Carrer, M., 2008. Age-dependent xylogenesis in timberline conifers. *New Phytologist* 177, 199–208.
- Ryan, M.G., Binkley, D., Fownes, J.H., 1997. Age-related decline in forest productivity: patterns and process. *Advances in Ecological Research* 27, 213–262.
- Ryan, M.G., Phillips, N., Bond, B.J., 2006. The hydraulic limitation hypothesis revisited. *Plant, Cell and Environment* 29, 367–381.
- Ryan, M.G., Yoder, B.J., 1997. Hydraulic limits to tree height and tree growth. *BioScience* 47, 235–242.
- Till, C., 1987. The summary response function of *Cedrus atlantica* (Endl.) Carrière in Morocco. *Tree-Ring Bulletin* 47, 23–36.
- Till, C., Guiot, J., 1999. Reconstruction of precipitation in Morocco since 1100 AD based on *Cedrus atlantica* tree-ring widths. *Quaternary Research* 33, 337–351.
- Touchan, R., Anchukaitis, K.J., Meko, D.M., Attalah, S., Baisan, C., Aloui, A., 2008. Long term context for recent drought in northwestern Africa. *Geophysical Research Letters* 35, L13705.
- Touchan, R., Xoplaki, E., Funkhouser, E., Luterbacher, J., Hughes, M.K., Erkan, N., Akkemik, U., Stephan, J., 2005. Reconstructions of spring/summer precipitation for the Eastern Mediterranean from tree-ring widths and its connection to large-scale atmospheric circulation. *Climate Dynamics* 25, 75–98.
- Vaganov, E.A., Hughes, M.K., Shashkin, A.V., 2006. Growth Dynamics of Conifer Tree Rings: Images of Past and Future Environments. Springer, Berlin, 354 pp.



738 van der Schrier, G., Briffa, K.R., Jones, P.D., Osborn, T.J., 2006. Summer moisture  
739 variability across Europe. *Journal of Climate* 19, 2818–2834.  
740 van Mantgem, P.J., Stephenson, N.L., Byrne, J.C., Daniels, L.D., Franklin, J.F., Fulé,  
741 P.Z., Harmon, M.E., Larson, A.J., Smith, J.M., Taylor, A.H., Veblen, T.T., 2009.  
742 Widespread increase of tree mortality rates in the western United States. *Science*  
743 323, 521–524.  
744 Voelker, S.L., 2011. Age-dependent changes in environmental influences on tree  
745 growth and their implications for forest responses to climate change. In:  
746 Meinzer, F.C., Lachenbruch, B., Dawson, T.E. (Eds.), *Size- and Age-related  
Changes in Tree Structure and Function*. Springer, Dordrecht, pp. 455–479.

Wharton, S., Schroeder, M., Bible, K., Falk, M., Paw, U.K.T., 2009. Stand-level gas-  
exchange responses to seasonal drought in very young versus old Douglas-fir  
forests of the Pacific Northwest, USA. *Tree Physiology* 29, 959–974.  
Yoder, B.J., Ryan, M.G., Waring, R.H., Schoettle, A.W., Kaufmann, M.R., 1994.  
Evidence of reduced photosynthetic rates in old trees. *Forest Science* 40,  
513–527.  
Zweifel, R., Eugster, W., Etzold, S., Dobbertin, M., Buchmann, N., Häsler, R., 2010.  
Link between continuous stem radius changes and net ecosystem productivity  
of a subalpine Norway spruce forest in the Swiss Alps. *New Phytologist* 187,  
819–830.

747  
748  
749  
750  
751  
752  
753  
754  
755  
756